

Received: 15 February 2022 / Accepted: 24 April 2022 / Published online: 04 May 2022

*industry 4.0, sensor,
machine behavior, forming machines*

Mohaned ALALUSS^{1*}, Robin KURTH¹, Robert TEHEL¹
Martin WAGNER¹, Nico WAGNER¹, Steffen IHLENFELDT^{1,2}

POTENTIAL OF TOOL CLAMPING SURFACES IN FORMING MACHINES FOR COGNITIVE PRODUCTION

High reproducibility of forming processes along with high quality expectations of the resulting formed parts demand cognitive production systems. The prerequisite is process transparency, which can be improved by increased knowledge of interdependencies between forming tool and forming machine that affects the tool clamping interface behavior. Due to the arrangement as surfaces transmitting process forces, their closeness to the forming process, and yet machine inherent, tool clamping interface provide greater potential for intelligent monitoring. This paper presents a holistic analysis of the interdependencies at the tool clamping interface. Here, the elastic deflection behavior of the press table and slide with their related clamping surfaces, the frictional slip behavior between the interacting machine components and the used clamping devices are described on qualitative level and verified by simulative analysis. Based on the results, available sensor systems are assessed regarding the capability to monitor the identified phenomena inline.

1. INTRODUCTION

The pursued goals of a climate-neutral, sustainable economy combined with the vision of zero waste manufacturing pose enormous challenges, especially for metal forming as an investment- and resource-intensive sector of serial and large-scale manufacturing of formed workpieces. Furthermore, productive operation is often dependent on optimum overall equipment effectiveness. Therefore, a transparency regarding the forming process and machine behavior is necessary to increase the overall equipment effectiveness by strongly reducing time for failure cause analysis, the tool try-out time and cost of forming tools [1]. An approach to generate the needed transparency is the use of monitoring systems based on sensors [2]. Depending on the target variables, different monitoring methods are known in the field of metal forming presses, which can vary from in-situ process [3] and condition monitoring [4] to end-of-line quality inspection as proposed in the work by Pierer et al. [5]. In addition, a basic classification can be made for monitoring into direct and indirect

¹ Department Machine Tool, Fraunhofer Institute for Machine Tools and Forming Technology IWU, Germany

² Chair of Machine Tools Development and Adaptive Controls, Dresden University of Technology TUD, Germany

* E-mail: mohaned.khaled.alaluss@iwu.fraunhofer.de

<https://doi.org/10.36897/jme/149414>

measurement principles regarding used inline monitoring systems. While direct measurement systems are known and often close-to-application as presented in the work by Biehl et al. [6], they are hardly applied in the metal forming sector due to high implementation effort (often these measurement systems are tool-bound) and the lack of robustness or the influence on machine properties (e.g. stiffness). These disadvantages do not affect indirect measurement systems, which predestines this type of data acquisition for a wide range of applications of various forming machines. However, to ensure an accurate and sensitive measurement as well as a robust inline monitoring during production operation, the knowledge of interdependencies between the forming tool and the forming press that affects the tool clamping interface behavior is indispensable. While individual aspects such as the deflection at the press table or the elastic deformation of T-slots are discussed in the scientific papers by Pilthammar et al. [7] and Kurth et al. [8], a holistic investigation of the interdependencies at the tool clamping interface is still missing.

Hence, the aim of this paper is to investigate the potential of tool clamping interface for inline process monitoring by describing the mentioned cause-effect relationships on qualitative level in Chapter 2 and verify them by simulative analysis in Chapter 3. In the following chapters, concepts for new and robust inline monitoring systems are developed and discussed based on the results obtained. Here, the achieved results allow the derivation of requirements for a robust and industry-usable sensor system. Additionally, available sensor systems are evaluated considering these requirements. In this context, the inline monitoring enables to acquire in-depth process and machine knowledge like the elasto-mechanical behaviour, which can be used as input data to enable more accurate simulations for process design in the future and a more load-oriented design of forming tools. This reduces the try-out time and cost for forming tools and therefore promises an increase in productivity. Moreover, this information can be used as a criterion to assess forming machines regarding their interchangeability during production with a specific forming tool or forming process, which improves flexibility in production planning. In addition, the obtained monitoring data offer potential benefits like the early detection of irregularities in process (e.g. changes in press force curve) and condition of the forming machine that can avoid unplanned machine downtimes. To conclude the contribution, a summary and outlook are given.

2. CHARACTERISTIC BEHAVIOR OF MACHINE CLAMPING SURFACES

During the manufacturing process, like the deep drawing process of large sheet metal workpieces (e.g. car bodywork), an elasto-mechanical deformation behavior of the forming tool and the interacting machine components (especially the forming tool, the tool clamping devices (e.g. clamping claw), the press table, the press slide and their clamping surfaces) can be observed, as illustrated in Fig. 1a.

Furthermore, the transmission of the process forces from the forming machine drive via the tool clamping surfaces to the forming tool results in a distribution of the acting reaction forces during the forming operation. This leads to elastic deformations of the mentioned machine components. The dependency of the elastic deformation on the magnitude of the

acting forces and its resulting two-dimensional distribution over the clamping surfaces can be adopted on the forming tool as stated in the work by Tehel et al. [9]. In this context, the elastic deformation of the interacting machine components can be characterized by the deflection behavior of the press table and press slide with their associated clamping surfaces, as shown in Fig. 1b. During the calibration of the final part contour, the inhomogeneous elastic deflection behavior causes considerable deviations in terms of homogeneous closing of the two forming tool halves (upper and lower die). Moreover, a frictional slip behavior of forming tool and machine clamping surfaces on each other is characteristically visible in the form of an elastic displacement of the forming tool compared to the press table and slide (Fig. 1c). These outlined effects have a negative impact on the resulting part quality and can be observed in the incorrect forming of geometric details, in unintended thinning of material and even in failure types like cracks, wrinkling and tearing. Therefore, to minimize the rejection rate of faulty parts, tool manufacturer and forming machine operators are die-spotting the forming tools, which is an experience-based and time-consuming process. Consequently, the elasto-mechanical machine behavior is of increasing importance in the try-out process and processes of production start-up as well as forming tool changes, which are underlined by the scientific works of Tehel et al. [9, 10], Pilthammar et al. [11] and Groche et al. [12]. Aside the global elasto-mechanical behavior of the machine clamping surfaces, the work by Kurth et al. [8] describes a local elasto-mechanical behavior in the form of the deformation of T-slots as integral elements on the machine clamping surfaces.

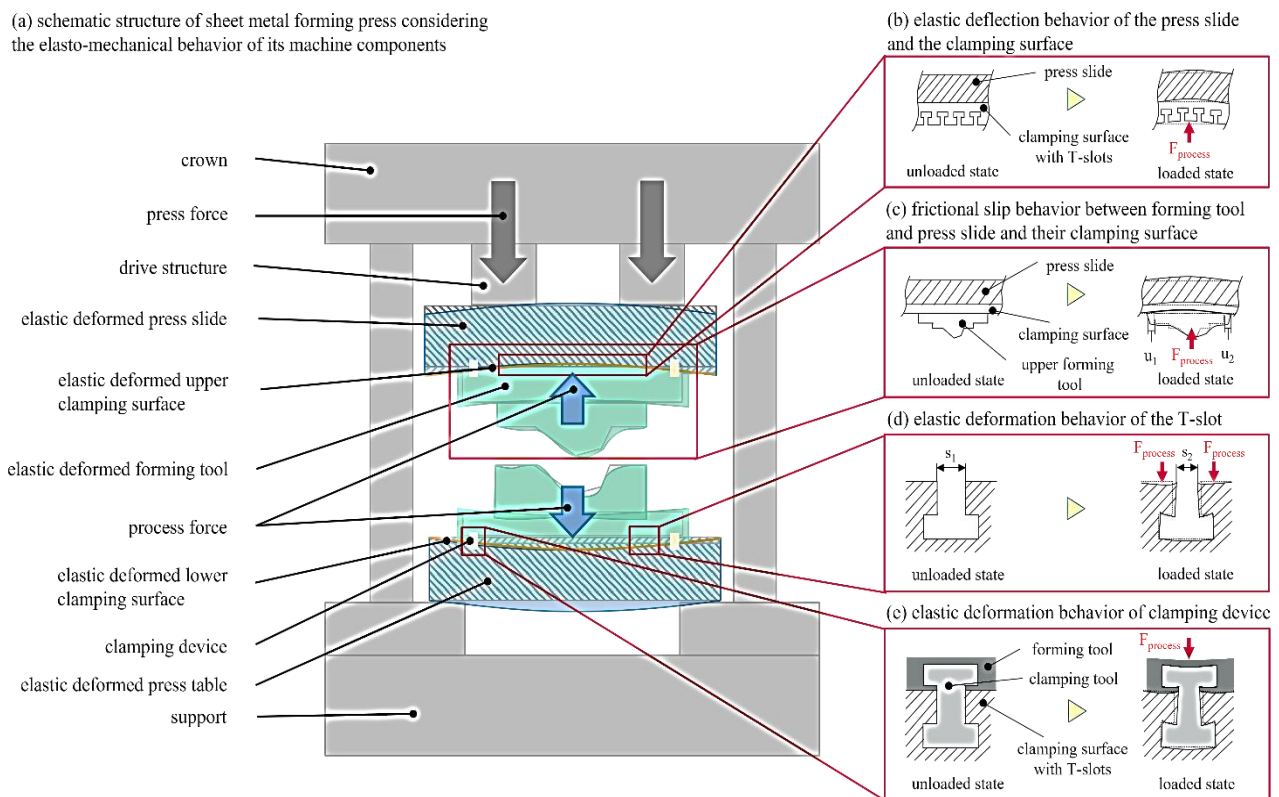


Fig. 1. Schematic representation of elasto-mechanical behavior of metal forming press – (a), elastic deflection of the press slide, the clamping surface – (b), frictional slip behavior of forming tool – (c), elastic deformation of the T-slot – (d), elastic deformation behavior of the used clamping devices – (e)

In Fig. 1d the elastic deformation of T-slot due to changes of the acting forces during the forming operation is presented. In addition, clamping devices are used to secure the forming tool in its position, whereby they also experience elasto-mechanical deformations due to changes in the acting forces, as shown in Fig. 1e. The work of Kurth et al. [13] demonstrate the approach of using elastic deformations of tool clamping devices to monitor process changes.

3. SIMULATIVE ANALYSIS OF THE ELASTO-MECHANICAL BEHAVIOR OF THE TOOL CLAMPING INTERFACE

The simulative analysis allows to understand the elasto-mechanical behavior and the cause-effect relationships by investigating the influence of the acting forces. In this paper, the focus will be set on the analysis of the press table, the lower forming tool, their clamping surfaces, and the associated clamping devices using the finite-element method (FEM) through the software ANSYS®. In this analysis, a 16 MN hydraulic forming press with mounted forming tool is used for the simulative investigations, as illustrated in Fig. 2a.

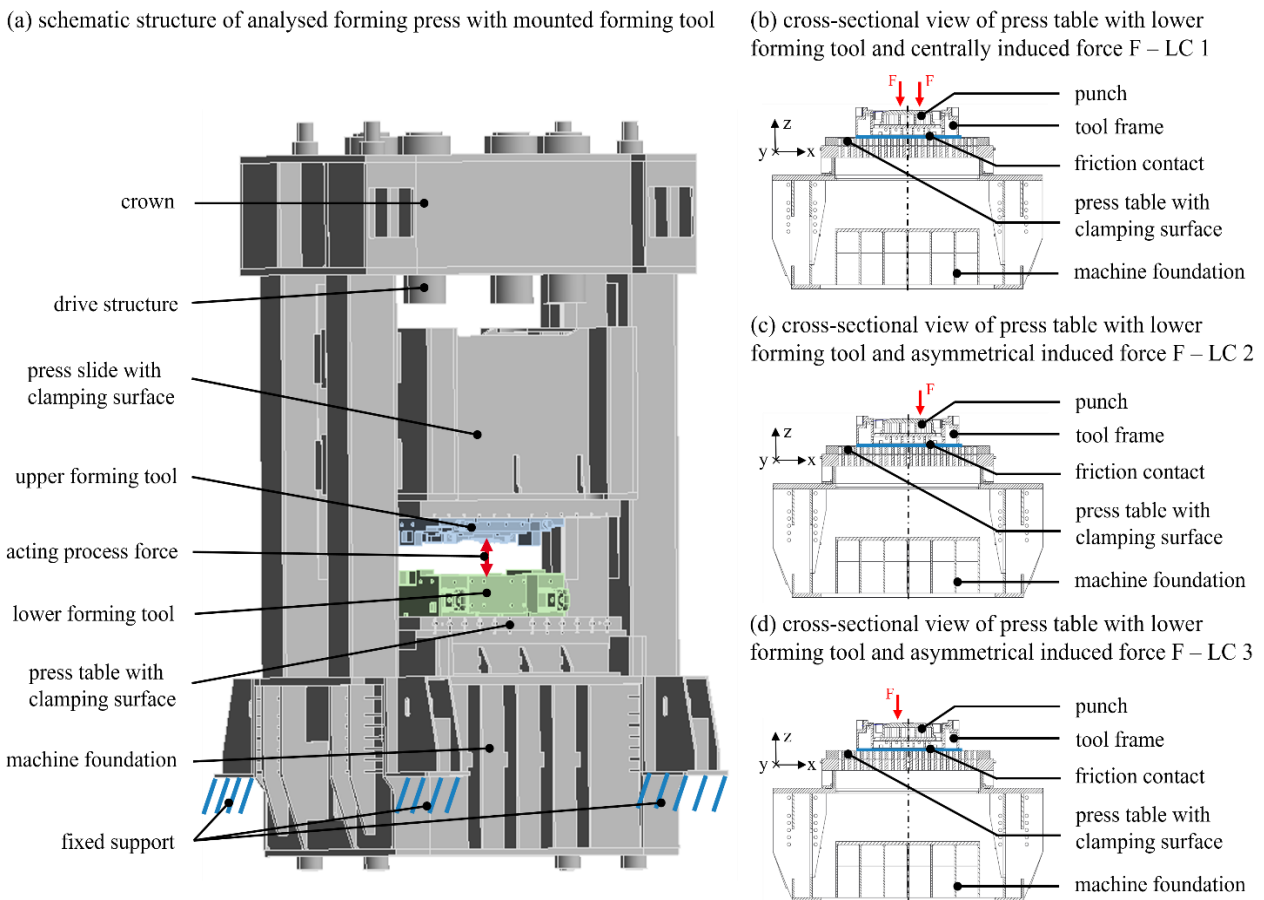


Fig. 2. Analyzed forming press with mounted forming tool – (a), defined load cases – (b) to (d) for the simulative analysis

Depending on the force magnitude and its location, varying load cases (LC) can be realized in the simulative analysis. As shown in Fig. 2b to 2d, three load cases are used where the acting force is induced through the punch. LC 1 represents a centric load case, whereas LC 2 and LC 3 both represent an eccentric load case with varying force magnitudes ($F_1 = 3 \text{ MN}$, $F_2 = 6 \text{ MN}$, $F_3 = 9 \text{ MN}$) for each of the three load cases. The LC 2 and LC 3 differ along the X-coordinate regarding the force application. Regarding the boundary conditions of the FE model, a fixed support of the machine foundation is defined. The machine components at the tool clamping interface, especially between the contact surfaces of the lower forming tool and the press table, are simulated with 1.0044 (S275JR) structural steel (elasticity modulus of 200000 MPa and Poisson's ratio of 0.3). Additionally, the contact area at the aforementioned tool clamping interface, is assumed to be a friction contact. Considering a steel/steel material contact for this area, the friction coefficient is set to 0.15. To keep the calculation time and memory consumption of the FE analysis appropriate, the mesh size is demand driven. Thus, only in the regions of the tool clamping interface and the contact areas a finer mesh is used whereas most of the structure fits fine with a relatively coarse mesh since only the dominant structural deflections are of interest.

3.1. DEFLECTION BEHAVIOR OF PRESS TABLE

Figure 3 shows the context between the resulting elastic deflection of the tool clamping surface of the press table under the defined LC 1 to LC 3 with the corresponding force magnitudes over the press table width (X-direction). As seen in Fig. 3a, the investigated elastic deflection trace ranges from $X_1 = -2000 \text{ mm}$ to $X_2 = +2000 \text{ mm}$ and lies in the press table center $Y = 0 \text{ mm}$.

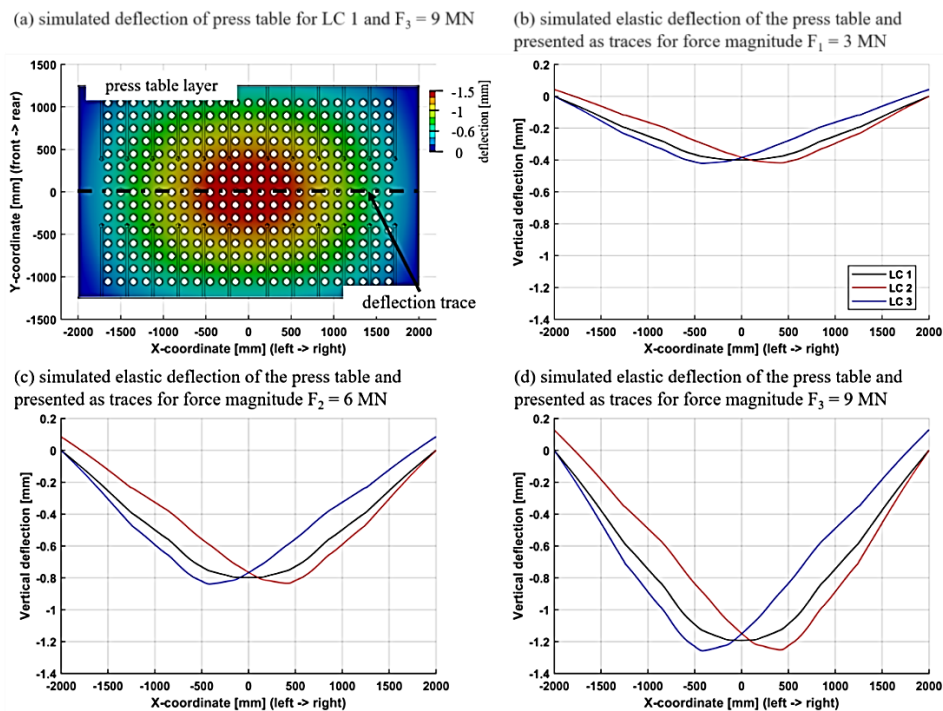


Fig. 3. Simulated elastic deformation results of the press table as traces considering LC 1 to LC 3

The direct comparison of the Figs. 3b to 3d shows a clear correlation between the induced force and the resulting elastic deflection of the tool clamping surface. The higher the magnitude of the acting forces, higher values of resulting elastic deflection are occurring. For LC 1 with the maximum force $F_3 = 9$ MN a maximum vertical deflection of -1.2 mm can be detected. Depending on the applied LC a shift relating to the position of the maximum elastic displacement along the X-coordinate can be seen. This shift clearly correlates with the respective force application areas in the forming tool. For the force magnitude $F_3 = 9$ MN, the position of the maximum elastic deflection for LC 2 can be registered at $X = +420$ mm and for LC 3 at $X = -420$ mm, which almost coincides with the defined force application areas.

3.2. FRICTIONAL SLIP BEHAVIOR BETWEEN FORMING TOOL AND FORMING MACHINE

During the forming operation, there is not only an elastic deformation of the tool interface components in the vertical direction, but also measurable elastic displacements in the horizontal direction can be observed, as shown in Fig. 4a. The simulated elastic deformation along the Y-coordinate over the entire tool width for LC 1 at the force magnitude $F_3 = 9$ MN is shown. As illustrated in Fig. 4a, not only the elastic displacement of the press table $u_{y,table}$ is analyzed but also the elastic displacement of the lower forming tool $u_{y,tool}$ in the contact layer of both components is investigated.

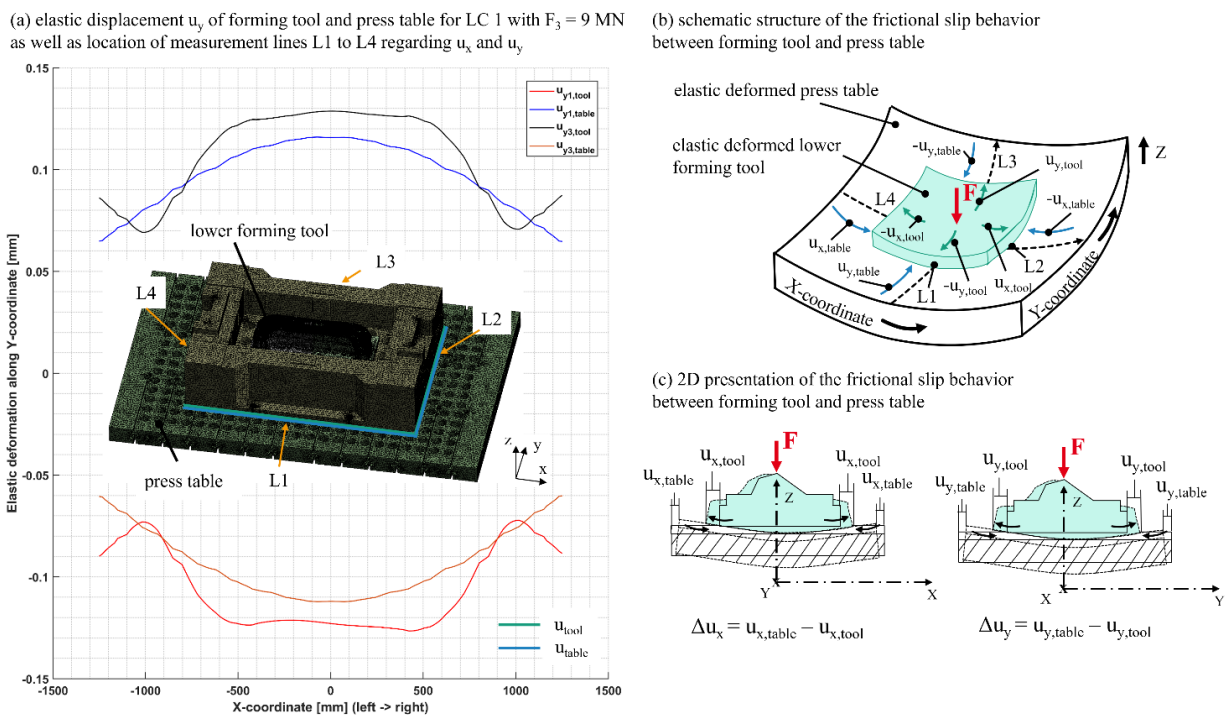


Fig. 4. Principle of the frictional slip behavior between lower forming tool and forming machine

The results for line L1 in Fig. 4a show exemplarily an elastic displacement regarding the press table with a maximum value of $u_{1y,table} = 0.12$ mm and for the elastic displacement

of the lower forming tool $u_{1y,tool} = -0.12$ mm. For the opposite L3, a tool displacement of $u_{3y,tool} = 0.13$ mm and a table displacement of $u_{y3,table} = -0.11$ mm could be determined simulatively. The results do not only show a difference in the elastic displacement of the examined components, but also that the respective directions of the elastic displacement of the press table and lower forming tool along the Y-coordinate are symmetrically opposing. This behavior is also visible along the X-coordinate (L2 and L4). Accordingly, a symmetrical distribution can be assumed for LC 1.

The described behavior is explainable by the acting shear stress in addition to the compressive stress due to the applied press force. Compared to the compressive stress, which mainly leads to the vertical deflection of the forming tool and the press table, the shear stress only contributes to a small extent to the elastic deformation of the tool clamping interface. The frictional contact between the lower tool and the press table, the different geometries of the components plus the acting shear stress result in the elastic slip behavior depicted in Fig. 4b and 4c. As already mentioned, the results for LC 2 and LC 3 are similar in general. Figure 5 depicts the influence of the force application on the elastic slip Δu at the tool clamping interface (Fig. 4c). Subsequently, the resulting elastic displacement along the Y-coordinate for the defined LC 1 to LC 3 with the corresponding force magnitudes is displayed for the L1 and L3. As described in Fig. 5a, the investigated measurement lines L1 and L3 are exemplarily shown for $Y = -800$ mm and $Y = 800$ mm.

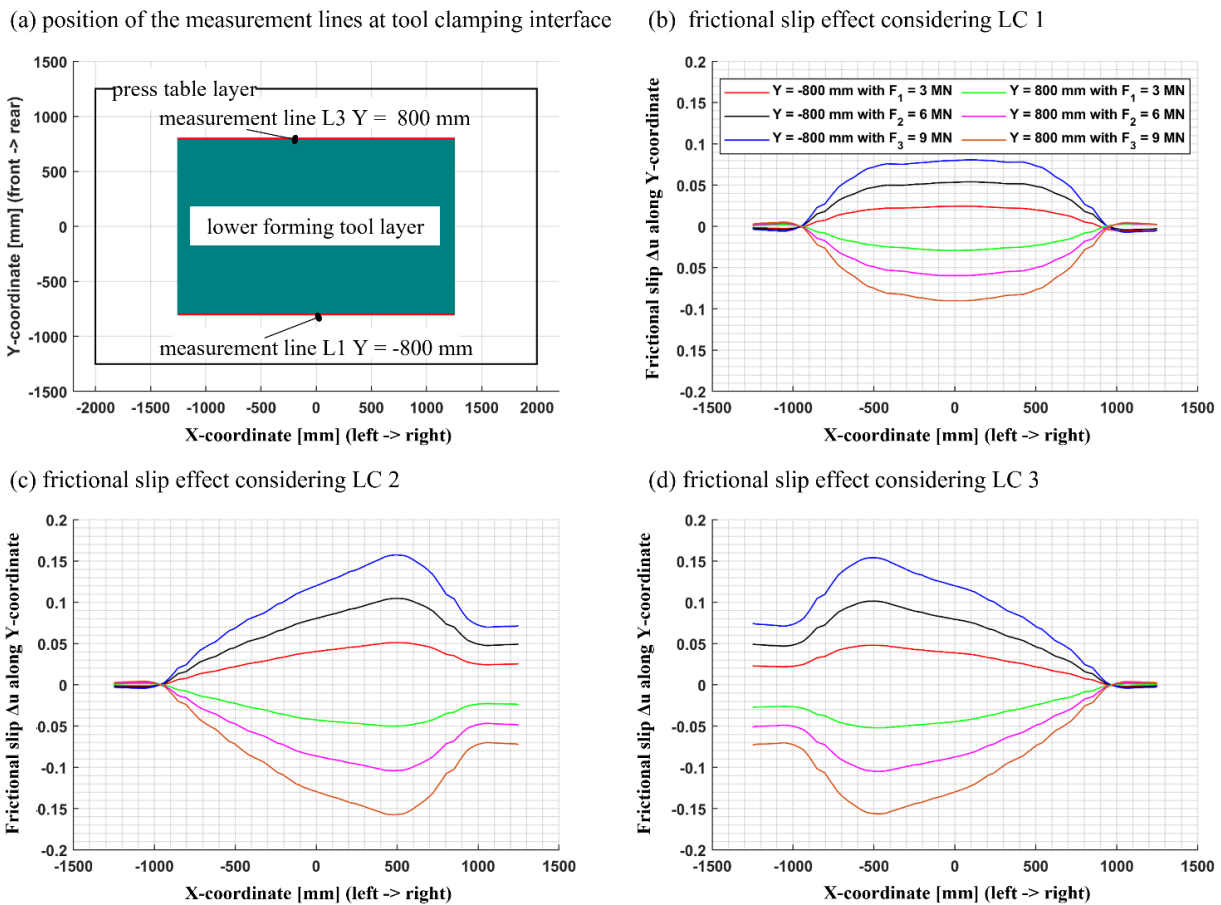


Fig. 5. Simulated frictional slip behavior between lower forming tool and press table considering LC 1 to LC 3

For LC 1 with the maximum force $F_3 = 9$ MN a maximum slip of 0.08 mm [$Y = -800$ mm] and -0.08 mm [$Y = +800$ mm] can be detected. However, the eccentric load cases LC 2 and LC 3 show higher slip values of ± 0.15 mm at F_3 and at $X = \pm 420$ mm. This confirms the shift relating to the position of the maximum along the X-coordinate depending on the applied LC. Moreover, from LC 1 to LC 3, the three frictional slip curves of L3 are qualitatively and in absolute value nearly identical to the three frictional slip curves of L1. Therefore, a symmetric behavior of the frictional slip curves can be clearly seen about $Y = 0$ mm. Thereby, the Y-coordinate defines the positions of measurement line L1 and L3.

3.3. DEFORMATION OF THE T-SLOTS Δs

The mentioned elastic deflection of the clamping surfaces on press table and slide are causing other elastic deformation effects in the machine structure. One of them is the elastic deformation of the T-slot geometry, which is typically used for clamping purposes of the forming tools inside the press. The elastic deformation of the T-slot geometry is mentioned in [8], where a basic analysis of the geometry behavior during standardized load scenarios is shown. Herein the general behavior is described as shown in Fig. 6 (a) by using the changes of the T-slot width $\Delta s = s_2 - s_1$ as characteristic value. Considering the thickness h of the clamping plate, Δs is depending on the Z-coordinate of evaluation.

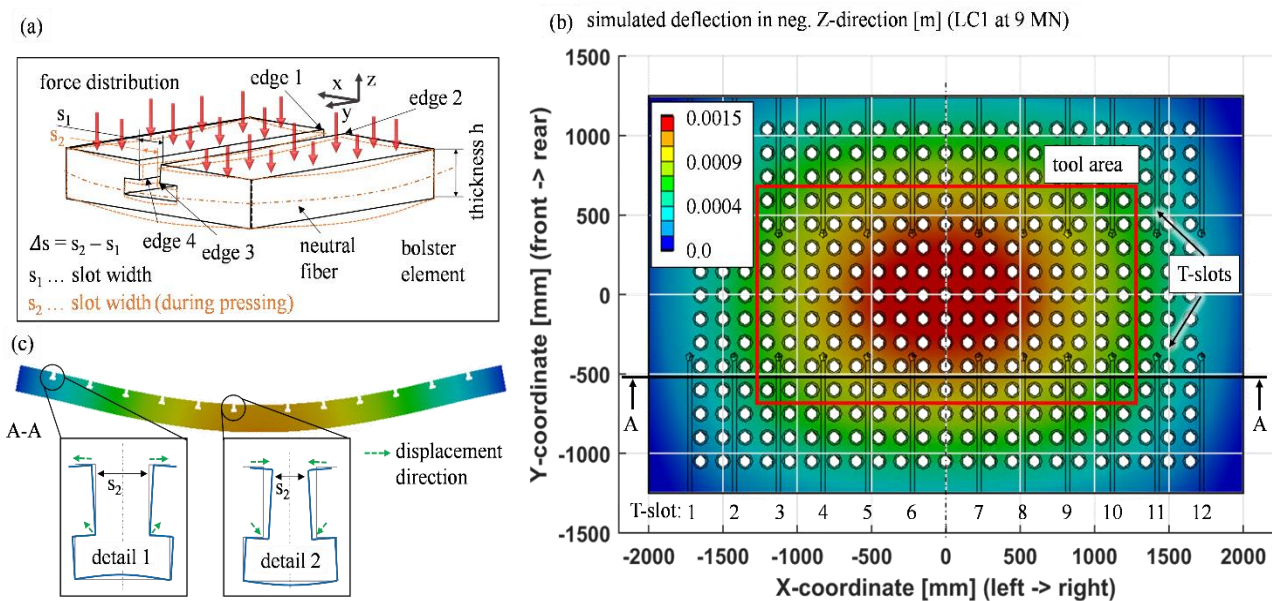


Fig. 6. General elastic deformation behavior of the T-slot [11] – (a), simulated elastic deflection of the clamping surface of the analyzed press (LC1, 9 MN) – (b), shapes of the resulting elastic deformation of the T-slot geometry – (c)

Following up this approach, within this paper the T-slot behavior is analyzed by FEM simulation applying real load scenarios by considering a forming tool and the FEM model depicted in Fig. 2. Figure 6b shows the resulting elastic deflection behavior of the clamping surface on the press table for LC 1 at acting force level F_3 . As depicted in both details in

Fig. 6c the elastic deformation of the T-slot geometry leads to positive (detail 1) and negative (detail 2) values of Δs in the analyzed case. The actual values of Δs are depending on its evaluation position characterized by the selected T-slot (numbers 1 to 12 in Fig. 6b) and Y-position in the T-slot. Within the following investigations, Δs is evaluated at the upper edges of the T-slot (edge 1 and 2 in Fig. 6a). The simulation results for all T-slots are depicted in Fig. 7. As it can be seen in Fig. 7a, the elastic T-slot deformation is depending on the distribution of the acting forces. In the diagrams, the differences of Δs as reaction on the load cases LC 1, LC 2 and LC 3 are noticeable and remain in measurable value ranges. It can be noted that the closer the T-slot is located at the center of the table (maximum elastic deflection) and the area of acting forces, the higher are the resulting values Δs . In general, a symmetrical behavior can be seen by applying LC 1. Focusing the simulation results applying LC 2 and LC 3, a shift of maximum values Δs can be seen.

Additionally, the elastic T-slot deformation is depending on the force magnitude, which can be exemplarily shown in Fig. 7b for T-slot 4. The diagram shows a strong dependency of the values Δs for the total T-slot length.

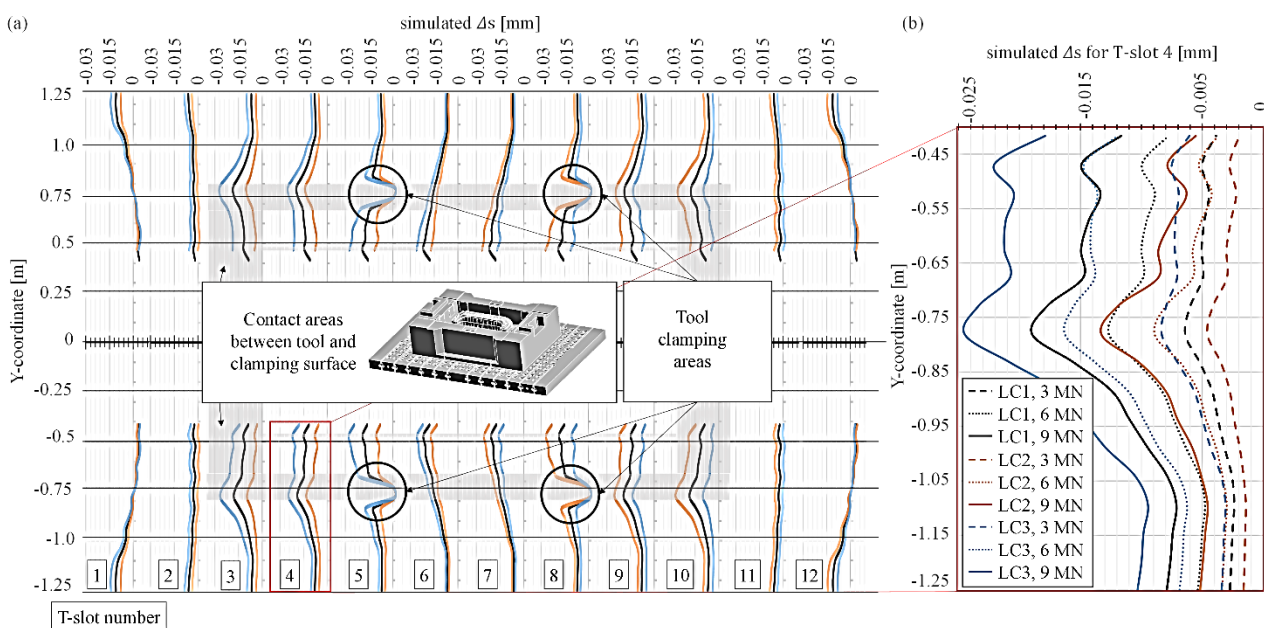


Fig. 7. Simulated values Δs for the T-slots on the clamping surface of the press table – (a), detail view of the simulated values Δs for T-slot 4 –(b)

With the focus on the simulation results, it can be stated that the elastic T-slot deformation reaches values in measurable ranges. However, the magnitude of the values Δs changes from T-slot to T-slot. Focusing the T-slots 2 and 11, nearly no elastic deformation ($\Delta s \approx 0 \mu\text{m}$) can be noted, whereas the T-slots 1 and 3 as well as 10 and 12 shows noticeable deformation (maximum $\Delta s \approx -30 \mu\text{m}$). This effect is mentioned in [8], where the deformation Δs is deduced as a representative parameter for the local curvature of the surface. Hence, the evaluation position must be considered to create a monitoring system. By using more than one measurement point, the global and local deformation shape of the T-slots can be

monitored. As depicted in Fig. 7a, the tool clamping situation and the tool contact geometry to the clamping surface also affects the elastic T-slot deformation locally.

3.4. ELASTIC DEFORMATION BEHAVIOR OF CLAMPING DEVICE

To analyze the occurring elastic deformations of the used clamping devices (CD) due to the application of process forces as in Sections 3.1 to 3.3, four CDs are implemented in the FE model and distributed as depicted in Fig. 8a. Here, a single CD is composed of the clamping screw, the washer, and the T-slot nut, as illustrated in Fig. 8b. Moreover, the material of CD is adopted as steel with a tensile strength grade of 8.8. Within the FE model the CD is connected to the lower forming tool by a defined bonded connection between the washer and lower forming tool surface to reduce the calculation effort. The contact areas between the T-slot nut of CD and the T-slot sides of the press table are modeled as friction contact areas (coefficient set at 0.15 due to a steel/steel material contact). Also, the contact area between the clamping screw in the thread area and the inner surface of the drilling in the T-slot nut is defined as frictionless contact during the pre-tensioning of CT at the beginning of the simulation and changed to a bonded contact before the process force is applied.

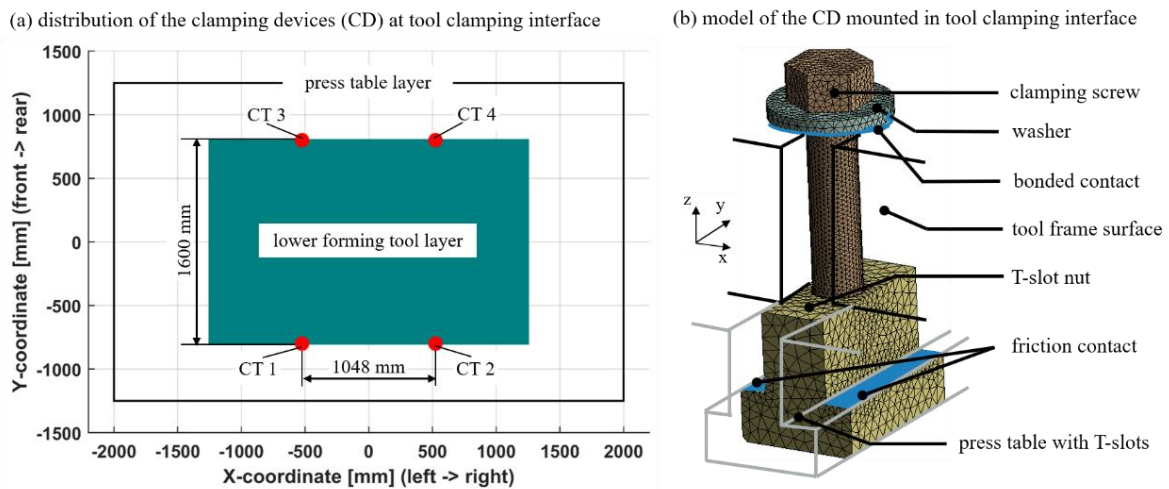
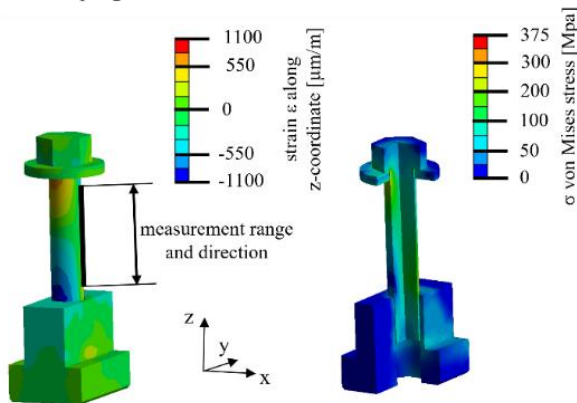


Fig. 8. Model structure of the clamping device (CD) and their positioning in the tool clamping interface

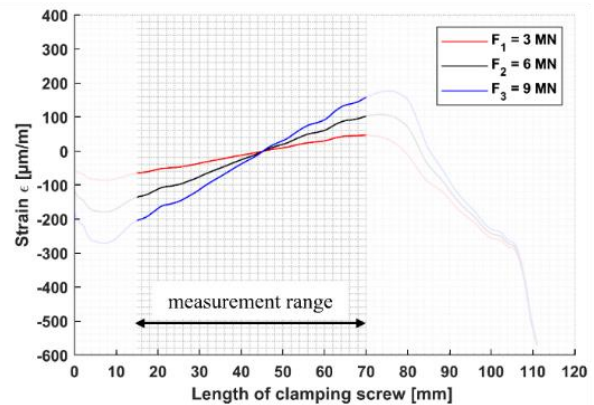
Specifically, the elastic deformation behavior is described using CT1 as an example and the corresponding results are presented below in Fig. 9. Thereby, the resulting normal strain distribution along the vertical axis Z and von Mises stress are shown in Fig. 9a for LC 1 with an applied force magnitude of $F_3 = 9$ MN. The strain value reaches $\epsilon_z = \pm 1100$ $\mu\text{m}/\text{m}$, which can be measured using classic strain gauges. Furthermore, Figs. 9b to 9d show the simulated normal strain change of the clamping screw for the three LC and their corresponding force levels F_1 to F_3 . In addition, the von Mises stress reaches values up to $\sigma = 375$ MPa, which is lower than the yield strength of 640 MPa. Therefore, these deformations can be interpreted as an elastic deformation of the CT1.

The values in these diagrams show linear behavior over length range from 15 mm to 70 mm of the clamping screw. The nonlinear strain behavior in the interval 0 to 15 mm reasons in the bonded contact between the clamping screw and the washer, whereas the nonlinear behavior in the range between 70 mm to 111 mm can be explained by the bonded contact of the thread.

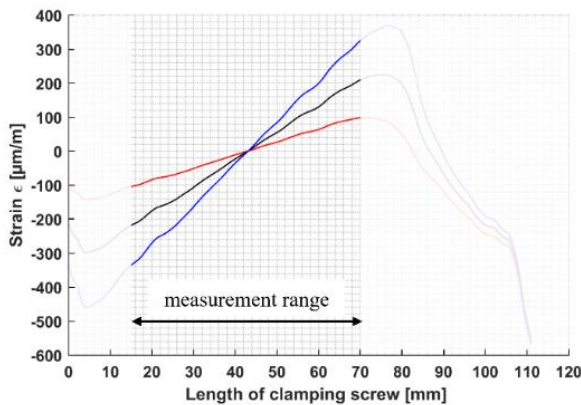
(a) simulated strain and von Mises stress distribution of clamping tool 1 for LC 1



(b) strain changes of the clamping screw shank for LC 1



(c) strain changes of the clamping screw shank for LC 2



(d) strain changes of the clamping screw shank for LC 3

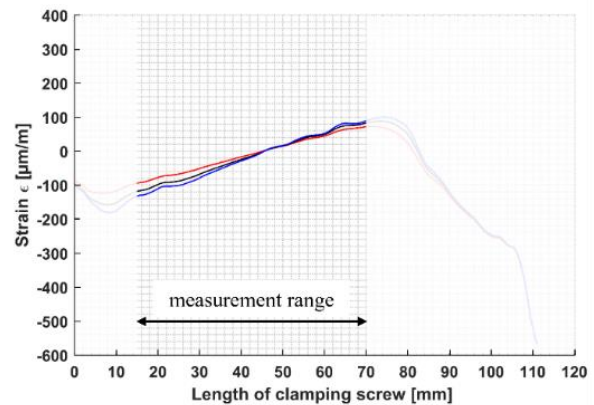


Fig. 9. Simulated strain changes of the clamping screw considering LC 1 to LC 3

Consequently, the length range between 15 mm and 70 mm is the focus of the data evaluation. Here, Table 1 summarizes the strain changes $\Delta\epsilon_z$ for the respective load cases and their associated force magnitudes F_1 to F_3 .

Table 1. Simulated strain changes $\Delta\epsilon_z$ of the clamping screw

Load case	Simulated strain change $\Delta\epsilon_z$ for $F_1 = 3$ MN	Simulated strain change $\Delta\epsilon_z$ for $F_2 = 6$ MN	Simulated strain change $\Delta\epsilon_z$ for $F_3 = 9$ MN
LC 1	110 $\mu\text{m/m}$	235 $\mu\text{m/m}$	350 $\mu\text{m/m}$
LC 2	195 $\mu\text{m/m}$	410 $\mu\text{m/m}$	640 $\mu\text{m/m}$
LC 3	160 $\mu\text{m/m}$	200 $\mu\text{m/m}$	220 $\mu\text{m/m}$

Besides the force magnitude, a strong influence regarding the position of the force application on the strain changes of the clamping screw is visible in the values of Fig. 9 and Table 1. With an eccentric load case like LC 2, higher strain changes compared to LC 1 are registered. However, the strain changes in the eccentric LC 3 are significantly lower than in LC 2. The reason is that the CT1 position, as depicted in Fig. 8a, is significantly closer to the acting forces area of LC 3 compared to the force application position of LC 2. Thus, in case of LC 2 the large normal strain changes result from the great scope in terms of frictional slip compared to closeness between CT1 position and LC 3. This behavior was also observed for CT3 as well as for CT2 and CT4 in the opposite direction.

4. SENSOR SYSTEMS FOR INLINE MONITORING AT TOOL CLAMPING INTERFACE

The core concept of monitoring is to record the exact status of a system by means of sensors and to initiate appropriate measures in the event of irregularities. Hence, it is not only essential to avoid machine downtimes, but also to maintain the specified product quality as well as to identify process deviations, as stated in the work by Kubik et al. [14]. However, the major challenge lies in an implementation of sensing technologies in complex manufacturing systems without restriction of the functionality or robustness of the regarded manufacturing machine.

The usability of sensor system in the forming machine environment can be assessed through requirements, which can be derived from the interdependencies between the changes of process force and the resulting changes of elasto-mechanical deformation of the tool clamping interface described in Chapter 2 and 3. Thereby, the key requirements can be summarized as follows: capability for inline monitoring, complexity, robustness as well as lifetime and adaptability. The capability for inline monitoring is linked with the ability of real-time continuous monitoring, which is necessary to enable trouble-free production operation. The core challenge lies in a measurement close to the impact location (high measurement accuracy and real-time capability) and, mechanically robust sensor integration for determining the elastic deformation of the press table and slide with their clamping surfaces. As already mentioned, the robustness of the sensor system and its integration without changing or affecting the geometric global shape of the forming machine and its components is an essential requirement. This results in demands for a high degree of insensitivity to production-related influences such as oils, cooling lubricants, dirt particles and high temperatures (depending on the forming technology). The adaptability of the sensor system is beneficial due to the great technological diversity and the large number of forming production systems in different technical development stages. In addition, the requirement for an operational lifetime of the used measuring systems can be derived from the production systems that have been in application for several decades. Besides the high reproducibility, accuracy and sensitivity of the measurement results, the complexity of the sensor system regarding the usage and commissioning is of enormous importance. Further on, several measuring points (depending on the sensor principle) are required not only to gather local information, but also to acquire global condition or process changes like the planar

manifestation of the deflection of press table and their associated clamping surfaces. Table 2 summarizes a variety of direct or indirect sensor and monitoring approaches associated with the clamping surfaces, which are evaluated based on the described key requirements.

Table 2. Assessment of existing sensor systems associated with tool clamping interface regarding application requirements (“●” = particularly high, “◐” = high, “◑” = medium, “◒” = low and “○” = extremely low)

Publ.	Target parameter	Measurement principle	Capability for inline monitoring	Complexity	Robustness / Lifetime	Adaptability	State of development
[13]	Local elastic deformation of clamping device	Usage of strain signals of intelligent tool-clamping device	◐	◑	◐	◐	◑
[7, 15]	Deflection of press table/slide	Optical camera devices to measure elastic deformations of press table or slide	○	◐	◐	◐	◑
[16]		Deflection measuring method based on fiber optic sensors	◑	◑	◐	◑	◑
[8]	Local elastic deformation of T-slot	Sensor device based on measuring strain in T-slot using a deformation body	●	◑	◐	●	◑
[17]		System consisting of eddy current sensors detecting deflection of the T-slot ground	◑	◐	◑	◑	◑
[18]	Reaction process force and their distribution	Sensor system between forming tool and tool-clamping surfaces of press table or slide	◐	◑	◐	◐	◑
[19]	Reaction process force	Pre-tensioning of a system consisting of piezo sensors on a press table	◐	◑	◐	◐	◐

In principle, the monitoring methods presented in [7, 15 – 16] are suitable for quantifying the deflection behavior and their distribution of press table and slide with the associated clamping surfaces. However, for the optical [7] or camera-based measurements [15], both the try-out process and the production process must be interrupted because an inline monitoring is not possible. In that regard, the area of the forming tool cannot be covered by these measuring systems due to their setup like the laser targets. This applies equally to the lately published work by Pilthammar et al. [16], which depicts a measurement method on the basis of fiber Bragg grating (FBG) sensors for detecting the deflection of press table consisting of a steel beam with integrated FBG sensor along the beam. Unlike the monitoring methods [7, 15] the capability for inline monitoring is still given around the forming tool area. Yet, using FBG sensors needs additional peripherals like light source, photoreceiver and complex electronic to evaluate the change in light level resulting from the force-dependent deformation. The high manufacturing costs and the technical preparation and adjustment of the FBG issue associated with this creates a negative impact.

The elastic deformation of the T-slots to changes of the acting press forces during the forming operation as proven in Chapter 3 are used as measurement principle in the works of [8] and [17]. In [17], the measurement approach is based on the usage of eddy current sensors to detect the deflection of the slot ground occurring during the forming process. The disadvantage of the proposed approach lies in the meagre robustness due to the eddy current sensors that requires high degree of environmental cleanliness which is almost impossible to achieve in forming technology. Furthermore, the adaptability is limited due to high complexity of the sensor system and the space requirement, where the sensor system fills at least one entire T-slot. On contrary to [17], the recently published scientific work [8] describes a less complex sensor device comprising of a metallic deformation body with a horizontally orientated conventional strain gauge. By pre-tensioning the system using an attached screw the sensor device is sufficiently compact to be integrated more than once inside one T-slot as well as under the forming tool during the forming process. With multiple measuring points in the T-slots of the press table and slide, not only local information can be acquired but also global condition or process changes resulting from untypical like eccentric load application or unacceptable loads on forming tools can be detected.

Additionally, the functional extension of conventional clamping devices by sensory functions, which is backed up by the simulative analysis in Section 3.4, can be seen in the scientific work of Kurth et al. [13]. This means there is necessarily no need to additional sensing technologies or even additional adjustment to forming machine or forming tool. Thereby, hydraulic-mechanical tool clamps are equipped with strain sensors to detect elastic deformation due to changes of the acting press forces during the forming operation. Depending on the machine and tool size, it is possible to use multiple clamping devices symbolizing multiple measuring points and therefore generates statements involving process changes. However, the benefits of the described intelligent tool clamping device can only be unleashed through data evaluation based on a model-based approach. Thus, the sensor signals of different clamping devices are transformed into information regarding the forming process.

In addition to the focus on the elastic deformations occurring in the tool clamping interface, there is the possibility to measure process forces transmitted from the forming machine via the machine clamping surfaces to the forming tool. In [18] a modular sensor system for recording the force distribution during a forming process is presented. This sensor system is arranged between the forming tool and the clamping surfaces of press table or slide. Furthermore, the single module combines the sensors in form of strain gauges and the electronics for data processing. Consequently, the implementation of the sensor system close to the process enables the detection of the acting press forces on the component during the forming process. Due to their closeness to the forming process, the capability for inline monitoring of the described sensor system can be assessed as high. The described measuring method is characterized by an influence on the forming machine properties, in particular the machine stiffness. At the same time, the installation of this sensor system leads to a reduction in the working space of the forming press and must be repeated with every tool change. This leads to a significant increase in tool exchange time and thus has a negative effect on the adaptability of the system. Furthermore, the company Unidor introduces a clamping system [19] for monitoring highly dynamic cumulative reaction process forces during stamping operations. By pre-tensioning of this system consisting of piezo sensors, the local curve of the forming

force can be monitored. Yet, with this system no statements can be made regarding the two-dimensional distribution of the reaction process forces.

While sensor systems for inline monitoring approaches related with the clamping surfaces exist in principle, their realization shows different development stages. Some systems, for instance [16] and [8], address partial action mechanisms such as the deflection behavior of press tables and the elastic deformation of T-slots, respectively. Nevertheless, the monitoring data show high potential for clarifying until little explored interdependencies like the slip behavior between the forming tool and the forming presses.

In summary, it can be stated that measuring systems as presented in [8] as well as clamping devices equipped with sensors have a high potential for inline process monitoring. The underlying active principles in the form of elastic deformation of T-slots and clamping devices have shown a high sensitivity with respect to the varying force magnitudes and application area in Chapter 3. Considering the high robustness due to the compact sizes of these systems enable a growth of process transparency and therefore are further modules towards cognitive production.

5. SUMMARY AND OUTLOOK

The presented investigations focused on the potential of the tool clamping interface in forming machines for inline process monitoring. The interdependencies between the forming tool and the forming press that affects the tool clamping interface behavior are described and divided into four core phenomena: the elastic deflection behavior of the press table and slide with their related clamping surfaces, the frictional slip behavior between forming tool and press table and slide, the elastic deformation of the T-slot and the elastic deformation of the used clamping devices to secure the forming tool. Considering load cases with different force application areas and force magnitudes, the mentioned phenomena are investigated by means of FEM simulations and evaluated regarding the potential for monitoring. Thereby, the simulative analysis shows a strong dependency between the force application areas as well as force magnitudes and the four described core phenomena (Section 3.1 to 3.4). The identified elastic deformations and displacements are remarkably high, which implies a high potential for inline process monitoring. On this basis, different sensor systems are assessed regarding key requirements derived from the analyses like the capability for inline monitoring, the accuracy as well as the industrial readiness. In this context, available systems like [16] or [8, 13] address already partial action mechanisms such as the deflection behavior of press tables, the elastic deformation of clamping devices and the elastic deformation of T-slots, respectively. However, to further improve the functionality of inline monitoring techniques the entire interdependencies between the forming tool and the forming press that affects the tool clamping interface behavior need to be considered, especially the frictional slip effect.

Future research works should focus on strengthening the simulatively obtained results by validating them with experimental investigations. Moreover, new sensor concepts considering the identified correlation must be developed and experimentally evaluated. These correlations must be further developed into algorithms for data analysis regarding process monitoring during forming operations.

ACKNOWLEDGEMENTS

This work was supported by the Fraunhofer High-Performance Center for Smart Production and Materials and by the Fraunhofer Cluster of Excellence Cognitive Internet Technologies CCIT.

REFERENCES

- [1] BEHRENS B.A., JAVADI M., 2009, *Exakte und Kostengünstige Qualitätskontrolle an Pressen in der Blechverarbeitungsindustrie*, UTF Science, Bamberg.
- [2] DOEGE E., SCHOMAKER K.-H., BRENDEL T., 1992, *Sensors and Diagnostic Systems in Forming Machines*, CIRP Annals 41/1, 323–336.
- [3] ZORN W., HAMM L., ELSNER R., DROSSEL W.-G., 2019, *Potential of the Force Distribution Measurement in Deep Drawing Processes for Increasing the Process Quality*, Int. J. Mech. Eng. Robot. Res. 8/3, 449–453.
- [4] IHLENFELDT S., RIEDEL M., WABNER M., TEHEL R., TISZTL M., FISCHER J., 2014, *Novel Maintenance Support System for Frame Components of Forming Presses*, European Congress & Expo on Maintenance and Asset Management (EuroMaintenance), Helsinki, 471–476.
- [5] PIERER A., WIENER T., GJAKOVA L., KOZIOREK J., 2021, *Zero-Error-Production Through Inline-Quality Control of Presshardened Automotive Parts by Multi-Camera Systems*, IOP Conf. Ser., Mater. Sci. Eng. 1157 012074.
- [6] BIEHL S., RUMPOSCH C., PAETSCH N., BRÄUER G., WEISE D., SCHOLZ P., LANDGREBE D., 2016, *Multifunctional Thin Film Sensor System as Monitoring System in Production*, Microsyst. Technol., 22, 1757–1765.
- [7] PILTHAMMAR J., SIGVANT M., HANSSON M., PALSSON E., RUTGERSSON W., 2017, *Characterizing the Elastic Behaviour of a Press Table Through Topology Optimization*, IOP Conf. Series, Journal of Physics, 896, 012068.
- [8] KURTH R., BERGMANN M., TEHEL R., DIX M., PUTZ M., 2021, *Cognitive Clamping Geometries for Monitoring Elastic Deformation in Forming Machines and Processes*, CIRP Annals Manufacturing Technology, 70/1, 235–238.
- [9] TEHEL R., PÄBLER T., MIHM M., 2019, *Modeling Elastic Behavior of Forming Machine Components to Reduce Tool Manufacturing Time*, Procedia Manufacturing, 27, 177–184.
- [10] TEHEL R., PÄBLER T., BERGMANN M., 2020, *Effective FE Models for Simulating the Elastomechanical Characteristics of Forming Machines*, Int. J. Adv. Manuf. Technol., 58/106, 3505–3514.
- [11] PILTHAMMAR J., SIGVANT M., KAO-WALTER S., 2018, *Introduction of Elastic Die Deformations in Sheet Metal Forming Simulations*, International Journal of Solids and Structures, 151, 76–90.
- [12] GROCHE P., HOPPE F., SINZ J., 2017, *Stiffness of Multipoint Servo Presses: Mechanics vs. Control*, CIRP Annals, 66/1, 373–376.
- [13] KURTH R., TEHEL R., PÄBLER T., PUTZ M., WEHMEYER K., KRAFT C., SCHWARZE H., 2019, *Forming 4.0: Smart Machine Components Applied as a Hybrid Plain Bearing and a Tool Clamping System*, Procedia Manufacturing, 27, 65–71.
- [14] KUBIK C., KNAUER S.M., GROCHE P., 2021, *Smart Sheet Metal Forming: Importance of Data Acquisition, Preprocessing and Transformation on the Performance of a Multiclass Support Vector Machine for Predicting Wear States During Blanking*, Journal of Intelligent Manufacturing, 23/5, 1489–1513.
- [15] Gesellschaft für Optische Messtechnik, 2010, *Application Note: 3D Motion Analysis: Optical Measuring Technology for Dynamic Analysis of Press Machines*, https://www.gom.com/fileadmin/-user_upload/industries/forming_machine_EN.pdf, Accessed on: 01 Nov. 21
- [16] PILTHAMMAR J., SKARE T., GALDOS L., FRÖJDH K., 2021, *New Press Deflection Measuring Methods for the Creation of Substitutive Models for Efficient Die Cambering*, IOP Conf. Ser., Mater. Sci. Eng. 1157 012076.
- [17] STRUCK R., 2010, *Bestimmung der minimal notwendigen Pressenkraft zur Herstellung von Karosseriestrukturbauteilen im Automobilbau*, PhD thesis, Leibnitz University, Hannover.
- [18] DROSSEL W.-G., ZORN W., HAMM L., 2019, *Modular System to Measure and Control the Force Distribution in Deep Drawing Processes to Ensure Part Quality and Process Reliability*, CIRP Annals Manufacturing Technology, 68/1, 309–312.
- [19] TESSARI K., 2016, *messQUADER mQ 5013.01. Der Allrounder zur Prozesskontrolle*, <https://www.unidor.info/assets/messquader-mq-5013.01.pdf>, Accessed on: 08 Dec. 21.